

Synthesis and characterization of carbon-coated magnetite for functionalized ferrouids

M. Arana¹, S.E. Jacobo², H. Troiani³ and P.G. Bercoff¹

¹Fa.M.A.F, Universidad Nacional de Córdoba. IFEG, Conicet. M. Allende s/n, 5000 Córdoba, Argentina

²LAFMACEL, Universidad de Buenos Aires. INTECIN, Conicet. Paseo Colón 850, C1063EHA Buenos Aires, Argentina

³Centro Atómico Bariloche - CNEA - CONICET, Instituto Balseiro, 8400 Bariloche, Argentina

Carbon-coated magnetite nanoparticles (NPs) were synthesized by the mechanochemical method in a high-energy ball mill using hematite and amorphous carbon as precursors. The milling was performed at 700 rpm, with a ball/powder mass ratio of 35 in stainless steel vials with WC balls and Ar atmosphere. The precursor powders were milled from 1 to 18 hours and they were annealed for 2 h in Ar at 500 °C. Structural and magnetic properties of the NPs were investigated by X ray diffraction (XRD), vibrating sample magnetometry and high resolution transmission electron microscopy (HRTEM). XRD patterns, refined with the Rietveld method, show that magnetite is present in samples milled from 6 hours onward and that after milling for 18 hours and annealing, the sample contains a single crystalline phase. Magnetization curves for samples with different milling times show saturation magnetizations ranging from 34.1 emu/g after 1 h to 78.0 emu/g after 18 h. Coercive fields are about 500 Oe for all samples. HRTEM studies reveal that the samples are made of amorphous carbon clusters with magnetite NPs less than or equal to 20 nm. This system seems appropriate for biomedical applications.

Index Terms—Carbon, Coatings, Magnetic nanoparticles.

I. INTRODUCTION

MAGNETIC FLUIDS made of iron oxides have several applications as magnetic inks, contrast media in medical imaging, transportation and release of drugs and hyperthermia [1,2]. For biomedical applications, the magnetic nanoparticles (NPs) must be coated with a biodegradable polymer [3,4] and then dispersed in the liquid carrier medium. The outer shell can protect the magnetic nanoparticles against environmental degradation. A ferrofluid of polymeric shells and magnetic cores used for transporting compounds to specific sites must possess certain properties: magnetic cores diameters equal or less than 20 nm and an appropriate magnetic response to external fields and to local gradients of the low rates found in biological systems [5].

High-energy ball milling is an appropriate technique for the synthesis of nano-sized particles. Mechanochemistry is the term applied to the process in which chemical reactions and phase transformations take place due to the application of mechanical energy [6]. This is a well-known process, with the first publication dating back to 1894 [7]. The applications of mechanochemistry include exchange reactions, reduction/oxidation reactions, decomposition of compounds, and phase transformations. Let M be a pure metal, R a reductant and MO an oxide reduced by R . Thus, the exchange reactions in mechanochemistry can be represented by an equation of the type $MO + R \rightarrow M + RO$.

In this work, activated carbon was chosen to reduce and coat ferritic NPs in order to functionalize them by adding a polymer.

II. EXPERIMENTAL

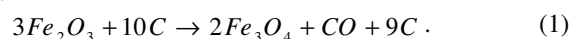
Magnetite (Fe_3O_4) NPs were synthesized by the mechanochemical method in a *Fritsch Pulverisette 7* high-energy ball mill. The samples' structural characterization was

performed by X ray diffraction (XRD) with a Phillip X'Pert diffractometer, with $Cu-K\alpha$ radiation, and Rietveld refinement using *FullProf Suite* software. The magnetic properties were determined with a Lake Shore 7300 vibrating sample magnetometer (VSM) at room temperature and with a maximum applied field of 1200 kA/m (1.5 kOe). The size distribution and the morphology of samples were investigated with a high resolution transmission electron microscope (HR-TEM) Philips CM 200 (200 kV).

III. SYNTHESIS AND STRUCTURAL CHARACTERIZATION

High-energy Ball milling

Hematite (Fe_2O_3) and activated carbon were used as precursors in a 4:1 mass ratio according to the following reaction:



As reaction (1) indicates, extra C is introduced in the vials so that a carbon excess remains in the sample even after the hematite reduction process has finished, covering the formed magnetite particles. An inert atmosphere had to be used in the milling vials to avoid secondary oxidation processes.

The milling was performed at 700 rpm, with a ball/powder mass ratio of 35, in stainless steel vials with WC balls and Ar atmosphere. Every synthesis parameter was chosen after several tests and previous studies.

The nomenclature for the samples resulting from the milling is set as CH-Ar- t . CH represent the precursors, carbon (C) and hematite (H); Ar indicates the milling atmosphere, t is the milling time in hours and takes the values 1, 2, 3, 6, 12 and 18.

Structural characterization and thermal treatments

X ray diffraction patterns of hematite and amorphous carbon used as precursors are shown in Fig. 1 and those of the resulting powders from the milling are shown in Fig. 2.

FIG. 1 HERE**FIG. 2 HERE**

From Fig. 2, it is evident that the expected chemical reaction (1) starts at $t = 6$ h, but hematite is still present in the powder even after milling for 18 hours (see Fig. 2), indicating that the reaction is not complete.

In order to get rid of the remaining hematite in the samples and avoid further milling, the samples were annealed in Ar for 2 h at 500 °C. This temperature was carefully selected to prevent a significant particle growth as well as C evaporation [8] while promoting hematite reduction.

The resulting powders after annealing were labeled CH-Ar-t-500. X ray diffraction patterns for these samples are shown in Fig. 3.

FIG. 3 HERE

It is clear from Fig. 3 that sample CH-Ar-18-500 contains a single crystalline phase because there are only magnetite reflections. Activated carbon is amorphous; therefore, no reflections arising from this phase are expected with this technique.

Rietveld analysis

X ray diffraction patterns were refined with the Rietveld method. Fig. 4 shows the fitting of the corresponding spectrum of sample CH-Ar-18-500.

FIG. 4 HERE

The structural parameters values for: cell parameter a , cell volume V , interplanar spacing d , density ρ and crystallite size $D_{crystal}$ were obtained from Rietveld refinement data and are shown in Table I for sample CH-Ar-18-500.

TABLE I HERE

Even when the Rietveld method is quite accurate for determining crystallographic parameters and phases, it has proven to be rather tricky when an amorphous material is present in the sample. So, even when obtaining values of χ^2 around 1 in every case, the overall quality parameter is high (indicating not a good overall fit). In order to take the amorphous fraction into account, a different approach to the refinement must be addressed. However, the parameters obtained for the crystalline phase (magnetite) are reliable.

IV. MAGNETIC CHARACTERIZATION

The specific magnetization (σ) as a function of the applied magnetic field (H) for samples CH-Ar-t and CH-Ar-t-500 was measured and it is presented in Fig. 5 and Fig. 6, respectively.

FIG. 5 HERE**FIG. 6 HERE**

While the σ vs. H curves of samples CH-Ar-t (for $t = 1, 2$ and 3 h) do not saturate and present low σ values (notice y-axis scaling in Fig. 5a), a significant increase in σ is observed when increasing the milling time from 1 to 3 hours (see Fig. 5a) This effect is due to the increase of the magnetite percentage with milling time. Samples milled from 6 to 18 hours do show a ferrimagnetic behavior (see Fig. 5b) as it is expected from the results obtained by XRD (Fig. 2) where magnetite starts to appear after 6 h of milling and increases with milling time, t .

On the other hand, all the σ vs. H curves of samples CH-Ar-

t-500 show a typical ferrimagnetic behavior (Fig. 6). The saturation specific magnetization (σ_s) of these samples takes the values presented in Fig. 7, where the σ_s values range from 34.1 emu/g after 1 h to 78.0 emu/g after 18 h (single phase sample).

The value of specific saturation magnetization for *bulk* magnetite σ_s' , is 92.5 emu/g, which is comparable to the specific saturation magnetization of sample CH-Ar-18-500 (78.0 emu/g). The difference can be attributed to the fact that sample CH-Ar-18-500 contains a fraction of carbon (non-magnetic material) apart from magnetite, so that σ_s is reduced. Besides, magnetization of a nanosized powder is usually reduced with respect to bulk magnetization values because of surface effects; in this case, the superficial chemical bonds are bound to be broken by the milling process and the annealing temperature is not high enough to restore them.

In every case, coercive fields are about 500 Oe. The powders display rather high coercivity values and a slow approach to saturation, indicating that the nanoparticles aggregate in clusters (as confirmed by TEM) with a wide dispersion of cluster dimension.

V. PARTICLE SIZES

Particle Size

The analysis of the particle sizes D_{parts} was performed using two methods:

1) *From HRTEM data*

HR-TEM micrographs show that crystalline NPs are embedded in carbon (see Fig. 8) both as single particles and clusters. Thus, a reactant agent is necessary in order to separate them before functionalizing.

FIG. 8 HERE

HR-TEM images also show that the particle size distribution is log-normal with an average particle size of 20 nm. This fact, together with the result from XRD indicates the existence of single crystal NPs.

2) *From magnetic data*

Chantrell *et al.* [9] introduced a mathematical expression for determining the average particle size, $D_{particle}$, and the corresponding standard deviation Δ using the magnetic parameters of samples, obtained from the σ vs. H curve and assuming spherical particles with a log-normal distribution. It is clear from Fig. 8, that Chantrell's expression can be used in this work.

Let T be the temperature at the moment of the VSM measurement, k_B the Boltzmann constant, χ_i the initial susceptibility, M_s the sample saturation magnetization, M'_s the bulk saturation magnetization and H_0 the coercive field. Then $D_{particle}$ and Δ can be calculated according to:

$$D_{particle} = \left[\frac{18k_B T}{\pi M'_s} \sqrt{\frac{\chi_i}{3M'_s H_0}} \right]^{1/3}, \quad (2)$$

$$\Delta = \frac{1}{3} \cdot \ln \left(\frac{3\chi_i H_0}{M_s} \right)^{1/3} \quad (3)$$

$D_{particle}$ and Δ were calculated using equations (2) and (3), the measured σ vs H curves of Figs. 5 and 6, and the samples densities from Rietveld refinement data. The resulting values for $D_{particle}$ at different milling times are shown in Fig. 9.

FIG. 9 HERE

Particle sizes of samples CH-Ar-t-500 decrease with increasing t because of the milling. The calculated value for $t = 18$ h is (15 ± 3) nm. This $D_{particle}$ is very close to the average particle size calculated from HRTEM images (20 nm). This result, together with the value of $D_{crystal}$ calculated in Section III (20 nm), lead to the conclusion that the obtained magnetite NPs are single crystal particles.

VI. CONCLUSIONS

Stable carbon-coated magnetite NPs at a room temperature were successfully synthesized by the mechanochemical method and further thermal treatment at 500 °C. A reduction of hematite to magnetite was induced by the mechanical process in which amorphous carbon was used in excess so as to remain covering the ferrite particles. The specific saturation magnetization of the resultant powder is very close to the bulk value. Crystal and particle sizes are the same (20 nm), indicating the obtention of single-crystal magnetite nanoparticles. An appropriate chemical reagent should be used to separate the carbon-coated single particles from clusters, before functionalizing the system for use in ferrofluids for biological applications. Preliminary results indicate that an appropriate mixture water-ketone (33%) satisfactory suspend the coated nanoparticles. Further experiences are in progress.

ACKNOWLEDGMENTS

This work was partially funded by Secyt-UNC and Conicet.

REFERENCES

[1] S. Odenbach, *Colloids and Surfaces A: Physicochem. Eng. Aspects*, vol. 217, pp. 171-178, 2003.
 [2] Y.M. Wang, X.Cao, G.H.Liu, R.Y.Hong, Y.M.Chen, X.F.Chen, *et al, J. Magn. Magn. Mater.*, vol. 323, pp 2953-2959, 2011.
 [3] T. Neuberger, B. Schöpf, H. Hofmann, M. Hofmann and B. von Rechenberg, *J. Magn. Magn. Mater.*, vol. 293, pp. 483-496, 2005.
 [4] V. Závřisová, M. Koneracká, M. Můčková, J. Lazová, A. Juríková, G. Lancz *et al, J. Magn. Magn. Mater.*, vol. 323, pp. 1408-1412, 2011.
 [5] A. Tomitaka, T. Koshi, S. Hatsugai, T. Yamada and Y. Takemura, *J. Magn. Magn. Mater.*, vol. 232, pp. 1398-1403, 2011.
 [6] C. Suryanarayana, E. Ivanov and V.V. Boldyrev, *Mater. Sci. and Eng.*, vol. A304-306, pp. 151-158, 2001.
 [7] M. Carry, *Phil. Mag.*, vol. 34, pp. 470-475, 1984.
 [8] M. Hisa, A. Tsutsumi and T. Akiyama, *Mat. Trans.*, vol. 45, No. 6 pp. 1907-910, 2004. R. Hussain, R. Qadeer, M. Ahmad and M Saleem, *Turk J. Chem.* vol. 24 pp 177-183, 2000.
 [9] R. W. Chantrell, J. Popplewell and S. W. Charles, *IEEE Trans. Magn.*, vol. 14, issue 5, pp. 975-977, 1978.
 [10] S. Bid and S.K. Pradhan, *Mater. Chem. Phys.*, vol. 84, pp. 291-301, 2004.
 [11] S. Bid, P. Sahu and S.K. Pradhan, *Physica E*, vol. 39, pp. 175-184, 2007.

TABLE I
RIETVELD REFINEMENT PARAMETERS FOR SAMPLE CH-AR-18-500

a ($\pm 0.0001 \text{ \AA}$)	V ($\pm 0.001 \text{ \AA}^3$)	d ($\pm 0.02 \text{ nm}$)	ρ ($\pm 0.01 \text{ g/cm}^3$)	$D_{crystal}$ ($\pm 0.02 \text{ nm}$)
8.3784	588.144	44.10	5.22	20.04

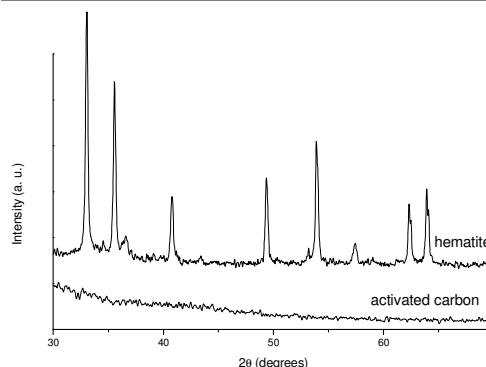


Fig. 1. X ray diffraction patterns of the selected precursors: crystalline hematite and amorphous carbon.

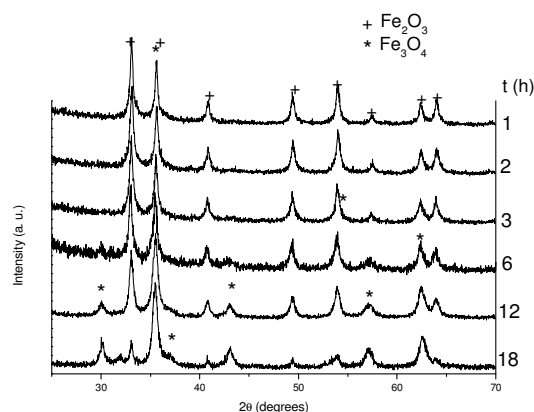


Fig. 2. X ray diffraction patterns for samples milled from 1 to 18 h. Hematite and magnetite reflection peaks are indexed with crosses and stars, respectively.

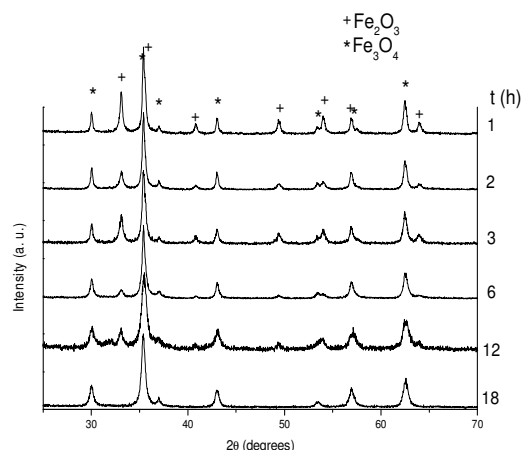


Fig. 3. X ray diffraction patterns for samples milled from 1 to 18 h and annealed for 2 h at 500°C in Ar atmosphere. Hematite and magnetite reflection peaks are indexed with crosses and stars, respectively.

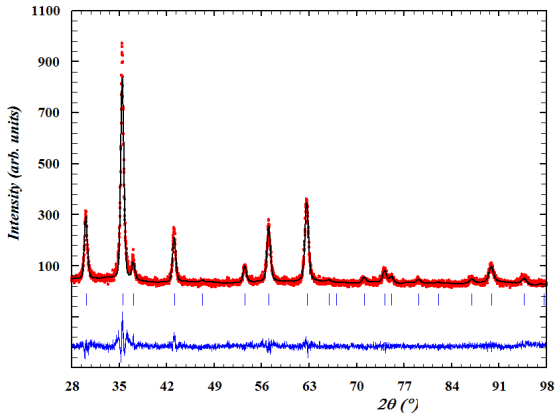
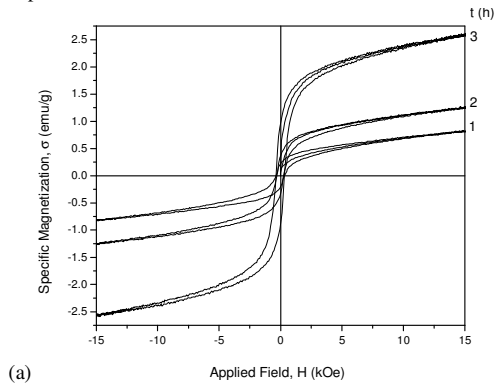
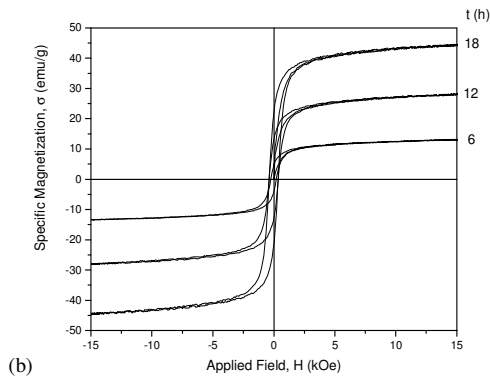


Fig. 4. Rietveld refinement of the XRD pattern of sample CH-Ar-18-500. Only magnetite reflections (vertical lines) are present in the pattern. Dots are experimental data, the dark line is the theoretical pattern and the line below is the difference between experimental and theoretical data.



(a)



(b)

Fig. 5. σ vs. H curves for samples CH-Ar-t; (a) $t = 1, 2$ and 3 h and (b) $t = 6, 12$ and 18 h.

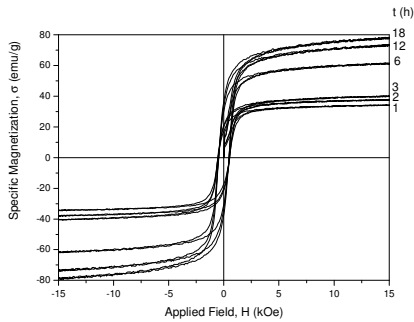


Fig. 6. σ vs. H curves for samples CH-Ar-t-500.

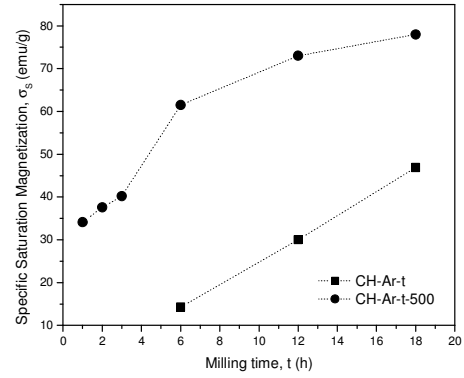


Fig. 7. σ_s vs. t for samples CH-Ar-t and CH-Ar-t-500.

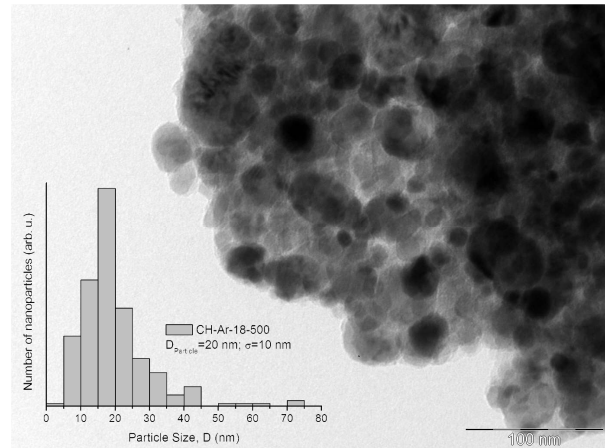


Fig. 8. HR-TEM image of sample CH-Ar-18-500. The inset shows the particle size distribution calculated from a set of images.

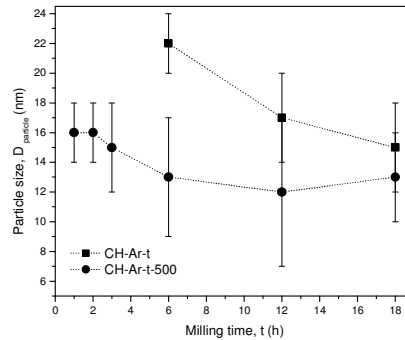


Fig. 9. Average particle sizes for samples CH-Ar-t-500 calculated with Chantrell's formula.